PAPER • OPEN ACCESS

Auger electron wave packet interferometry on extreme timescales with coherent soft x-rays

View the article online for updates and enhancements.

Auger electron wave packet interferometry on extreme timescales with coherent soft x-rays

Sergey Usenko[1,2,7], David Schwickert[1], Andreas Przystawik[1], Karolin Baev[2], Ivan Baev[2], Markus Braune[1], Lars Bocklage[1,3], Marie Kristin Czwalinna[1], Sascha Deinert[1], Stefan Düsterer[1], Andreas Hans[4], Gregor Hartmann[4,6], Christian Haunhorst[5], Marion Kuhlmann[1], Steffen Palutke[1], Ralf Röhlsberger[1,3], Juliane Rönsch-Schulenburg[1], Philipp Schmidt[4,7], Slawomir Skruszewicz[1], Sven Toleikis[1], Jens Viefhaus[6], Michael Martins[2], André Knie[4], Detlef Kip[5] and Tim Laarmann[1,3,*]

[1] Deutsches Elektronen-Synchrotron DESY, Hamburg, Germany
[2] Department of Physics, University of Hamburg, Hamburg, Germany
[3] The Hamburg Centre for Ultrafast Imaging CUI, Hamburg, Germany
[4] Institute of Physics, University of Kassel, Kassel, Germany
[5] Faculty of Electrical Engineering, Helmut Schmidt University, Hamburg, Germany
[6] Helmholtz-Zentrum Berlin für Materialien und Energie, Berlin, Germany

E-mail: tim.laarmann@desy.de

CrossMark

Abstract

Wave packet interferometry provides benchmark information on light-induced electronic quantum states by monitoring their relative amplitudes and phases during coherent excitation, propagation, and decay. The relative phase control of soft x-ray pulse replicas on the single-digit attosecond timescale achieved in our experiments makes this method a powerful tool to probe ultrafast quantum phenomena such as the excitation of Auger shake-up states with sub-cycle precision. In this contribution we present first results obtained for different Auger decay channels upon generating L-shell vacancies in argon atoms using Michelson-type all-reflective interferometric autocorrelation at a central free-electron laser photon energy of 274.7 eV.

Keywords: Auger effect, inner-shell excitation, free-electron lasers

(Some figures may appear in colour only in the online journal)

1. Introduction

The Auger effect is the emission of a secondary electron in the non-radiative decay of a core-hole excitation [1]. Auger electrons carry rich information about the electronic structure and dynamics of atoms, molecules, and solids, thus Auger electron spectroscopy has found prevalent application in the detailed study of atomic and molecular quantum systems and material sciences for a long time. Of course, Auger electrons are not monoenergetic. The fast decay of the excited core-hole states of the order of a few femtoseconds or even attoseconds leads to spectral widths in the range of a few tens of meV to several eV. For decades, the characteristic time constants describing the core-hole relaxation dynamics have

---

Figure 1. Experimental scheme for phase-sensitive electron wave packet interferometry in argon atoms induced with 274.7 eV photons. The photon energy autocorrelation of single-spike FEL shots used to record the present data set is shown in the inset.

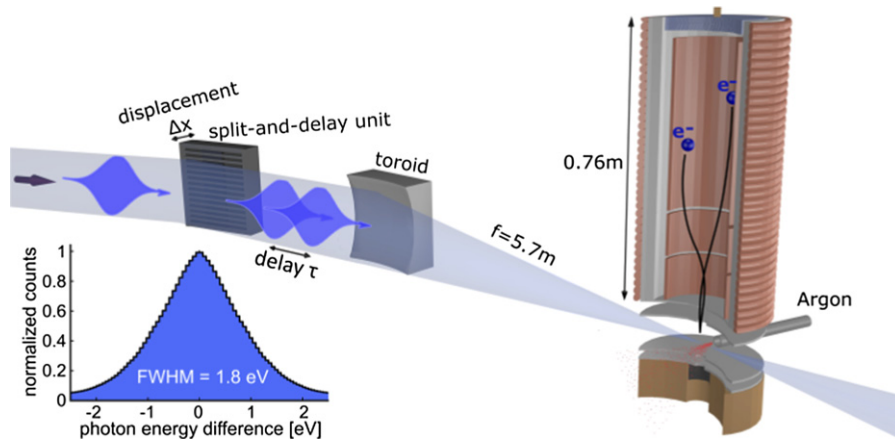been derived from the linewidth of electronic transitions using continuous-wave extreme ultraviolet (XUV) or x-ray spectroscopy. Meanwhile, the development of novel light sources and corresponding spectroscopic tools has enabled scientists to study ultrafast phenomena directly in the time domain on a time scale of less than a femtosecond [2, 3].

A hot topic in modern attosecond science is the investigation of the so-called Eisenbud–Wigner–Smith time delay, which is a measure for the spectral variation of the scattering phase [4]. In simple words, this is the time interval in photoemission between the absorption of a photon and the emission of an electron into the continuum. This quantity depends on the kinetic energy and the emission angle of the outgoing electron wave packet [5]. In the past, photoemission delays [6–11] were measured either by 'attosecond streaking' [12] or with the so-called 'attosecond clock' technique [13–16] and 'RABITT' (reconstruction of attosecond beating by interference of two-photon transitions) [17, 18]. All of these methods rely on optical laser fields (IR-VIS) synchronized with extreme precision to a short-wavelength pulse or pulse train used for photoionization. This is the realm of high-harmonic generation providing attosecond XUV and soft x-ray (SXR) pulses that are naturally synchronized to the optical drive laser. The full characterization of the emitted photoelectron wave packet in the presence of the optical field must go hand-in-hand with theoretical calculations to reconstruct the Eisenbud–Wigner–Smith time delay from the experimental data. It is important to note that in general, the optical laser field modifies the spectral variation of the scattering phase (delay) [4], which can only be corrected with the help of theory. Very recently, a new correction-free interferometric method using two phase-locked XUV pulses from the free-electron laser FERMI in Trieste was applied to clock attosecond delays in the photoemission from neon atoms [5]. The experimental results are in excellent agreement with theory. In the present contribution, we describe experiments at the SXR free-electron laser facility in Hamburg (FLASH) striving to clock SXR induced Auger electron emission from the decay of excited core-hole states in argon atoms in the time domain. The structural change of the electronic system

is a pure manifestation of electron correlation since it cannot be understood in terms of an effective one-electron model [19]. We used electron wave packet interferometry to measure relative phase shifts of different Auger and direct photoionization channels on the attosecond time scale upon generating an L-shell vacancy ($L_{2,3}$).

2. Experiment

A coherent SXR pulse of a few fs duration and photon energy of 274.7 eV ionizes a 2p electron from the corresponding L-subshell of argon atoms. Before the interaction with the sample the FEL pulses are split into two replicas, which are delayed with respect to each other using a Michelson-type all-reflective interferometric autocorrelator [20]. The compact device provides collinear propagation of both pulse replicas and thus constant relative phase difference across the beam profile. This enables to record phase-resolved autocorrelation signals with maximum contrast [21]. The experiment was carried out at the FL24 beamline of the FLASH2 free-electron laser (FEL) at DESY in Hamburg [22]. The schematic setup is shown in figure 1.

Ionization of an argon atom with a 274.7 eV photon produces a 2p core hole, which is predominantly refilled via Auger decay as depicted in the inset of figure 2. We omitted possible decay channels into triply and quadruply charged argon ions in the relaxation scheme, because their contribution to the total relaxation cascade upon photoionization from the 2p subshell is below 15% [23]. We also omitted transitions into $2p^{-1}3p^{-1}np$ satellite states of the di-cation with binding energies around 275 eV [24], which is slightly above the excitation photon energy.

The photoelectrons and Auger electrons created in the interaction region were detected by a microchannel plate (MCP) detector in a magnetic-bottle type time-of-flight (TOF) electron spectrometer. The MCP signal was digitized by a fast analog-to-digital converter and stored in the FLASH data acquisition system. The electron kinetic energies were calibrated with the well-known SXR induced electron emission from argon atoms.
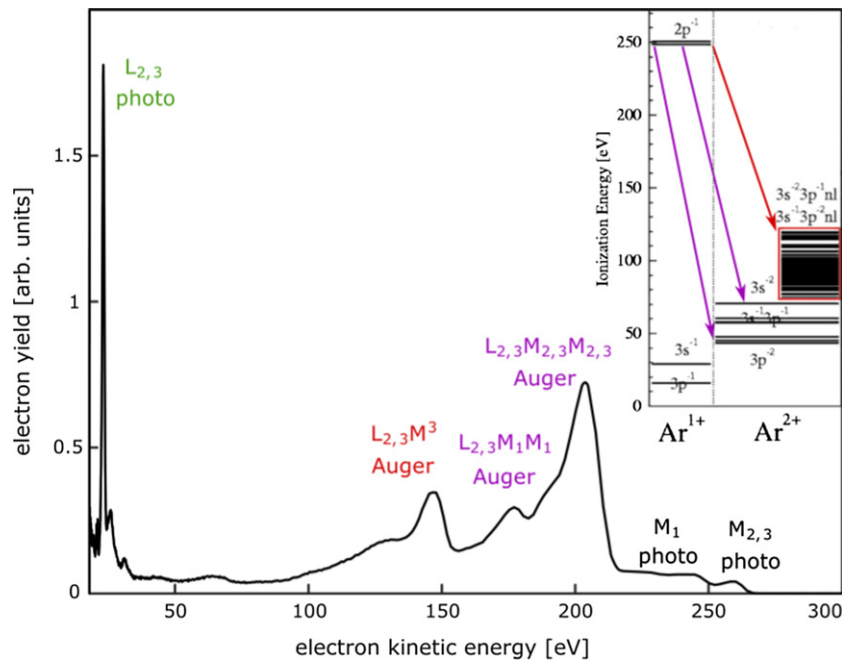
J. Phys. B: At. Mol. Opt. Phys. **53** (2020) 244008

S Usenko *et al*

Figure 2. Argon electron spectrum recorded at 274.7 eV photon energy. The energy level scheme based on single-configuration Hartree–Fock calculations including dominant Auger decay channels adopted from [23] is shown in the inset.

3. Results and discussion

The static electron spectrum using single-spike FEL pulses characterized by a high degree of longitudinal coherence with a central photon energy of 274.7 eV is shown in figure 2. Photoionization bands from M_1-, $M_{2,3}$- and $L_{2,3}$-subshells are clearly visible. In addition, characteristic $L_{2,3}MM$ Auger multiplets resulting from the decay of the $2p^{-1}$ hole state are observed. Non-radiative transitions into 'shake-up' states with an additional 'spectator hole' in the M-shell are observed as well. The corresponding transitions are labeled as $L_{2,3}M^3$.

The presence of open shells in the initial cationic as well as the final di-cationic states leads to a rather congested spectrum. The additional hole in the shake-up states changes the screening and thereby causes characteristic shifts of the transition energy, which give rise to so-called vacancy satellites in the spectrum. Moreover, the modified angular momentum coupling of the charge vacancies results in a more complicated multiplet splitting.

A rather simplified picture of the electronic states relevant for the decay of the $2p^{-1}$ hole states is presented in the inset of figure 2. The energy level scheme is based on single-configuration Hartree–Fock (SC-HF) calculations adopted from [23]. Note that the relative intensities of the experimentally observed Auger channels do not represent the transition probabilities because of the energy dependent transmission of the magnetic bottle spectrometer in the present setup.

First insight into correlated electron dynamics on the extreme single-digit attosecond time scale is obtained by the detection of Auger lines in the kinetic energy spectrum of emitted electrons as a function of pump-probe delay with interferometric contrast. Here, the high degree of

longitudinal coherence of single-spike FEL pulses and the unprecedented relative-phase control provided by our SXR autocorrelator are essential. Figure 3 shows the result of the electron wave packet interferometry recorded in a ≈120 attosecond scan range. Here, we counted the electrons falling into an energy bin of 0.3 eV width and plotted the electron yield as a function of delay between 'pump' and 'probe' SXR pulses in ≈1 attosecond steps. The key finding from the direct comparison of different simultaneously measured electron emission channels is that specific relaxation cascades, namely the $L_{2,3}M^3$ satellite transitions, show a relative time (phase) delay of approximately 3 attoseconds with respect to the oscillation of the driving SXR light wave. Natural references for the latter is given by the $L_{2,3}$ photoline. Its time dependence reflects the oscillation of the total energy in the interaction area due to the interference of the FEL field occurring when the relative phase between two pulses is varied with subcycle precision. The electron yield is thus proportional to the field autocorrelation trace, which has a period of ≈15 attoseconds corresponding to the duration of the optical cycle at the carrier wavelength 4.5 nm (274.5 eV). The delay-dependent yield of this photoline is plotted at the bottom of figure 3. It can be clearly seen that the formation of the 'normal' $L_{2,3}M_{2,3}M_{2,3}$ Auger multiplet structure (without spectator hole) follows the light wave oscillation in phase (at top), whereas the spectator decay into final shake-up states ($L_{2,3}M^3$) exhibits a clear phase shift (middle).

A simple way to describe LMM Auger decay processes in the time domain is to solve a rate equation model that determines the probability $P(t)$ to find the 2p hole at time t in an argon atom. It is given by the convolution of the SXR FEL pulse intensity distribution with the exponential Auger decay
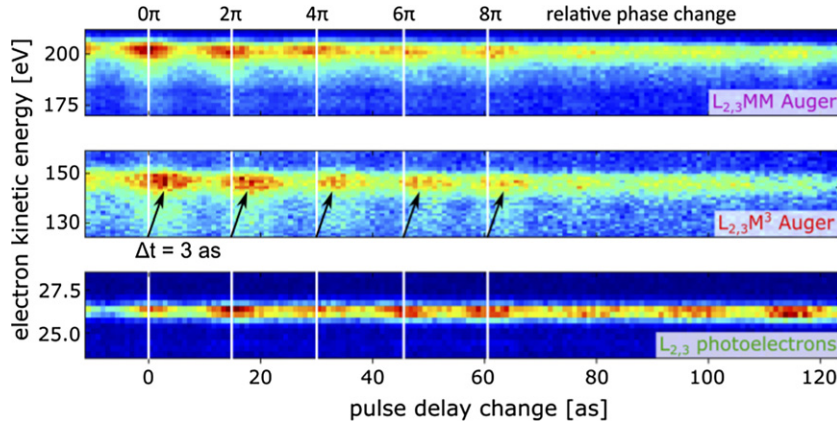
Figure 3. Interferometric traces of electron emission for different kinetic energies of ejected electrons. Each panel is normalized to its maximum and to the number of FEL shots per delay. The plotted ∼120 attosecond scan range corresponds to absolute time delays between the pulse replicas from ∼140 as to ∼260 as.

of $\Gamma = 112$ meV width [25].

$$P(t) = \frac{\sigma}{\omega_{\text{FEL}}} \int_{-\infty}^{t} I_{\text{FEL}}(t') \, e^{-\Gamma(t-t')} \, dt' \qquad (1)$$

Here, the absorption cross-section σ is assumed to be constant across the spectral bandwidth of the FEL pulse with the central angular frequency ω_{FEL} and intensity $I_{\text{FEL}}(t')$. However, this model does not include the phase relation of two ejected electron wave packets in a single-color FEL pump-probe scheme and thus is unable to describe interference effects in the present experiment [26].

Recently, Auger electron interference induced by XUV attosecond twin pulses has been treated theoretically by applying *ab initio* formalism for the quantum dynamics of inner-shell ionized krypton atoms [27]. In a so-called essential-states model, that considers only the absolutely necessary energies and matrix elements, the quantum-mechanical phases of propagating electronic wave functions are taken into account. The quantum dynamics of the inner-shell hole formation with subsequent Auger decay is described by equations of motion [26–28]. By adapting this formalism to the present SXR-FEL pump-probe scheme one obtains the probability density amplitude to detect a photoelectron with momentum $\vec{k}_{\text{P}}$ in coincidence with an Auger electron with momentum $\vec{k}_{\text{A}}$ in the final state as a function of delay τ between the two pulse replicas. It reads

$$\bar{c}_{\text{f}}^{\vec{k}_{\text{P}}\vec{k}_{\text{A}}}(\tau) \propto i\bar{d}\left(\vec{k}_{\text{P}}\right) \bar{q}\left(\vec{k}_{\text{A}}\right) \cdot s\left(\tau, \frac{k_{\text{P}}^2}{2m}, \frac{k_{\text{A}}^2}{2m}\right) \qquad (2)$$

with the dipole and Auger matrix elements $\bar{d}$ and $\bar{q}$, respectively. The matrix elements are slowly varying functions of $\vec{k}_{\text{P}}$ and $\vec{k}_{\text{A}}$ in the absence of resonances. significantly above the 2p ionization threshold. The two-electron line shape function is given by

$$s\left(\tau, \frac{k_{\text{P}}^2}{2m}, \frac{k_{\text{A}}^2}{2m}\right) \propto \frac{\tilde{\mathcal{E}}_{\text{FEL}}\left(\tau, \frac{k_{\text{P}}^2}{2m} + \frac{k_{\text{A}}^2}{2m} - \Omega_{\text{FEL}} - E_{\text{a}} - E_{\text{b}}\right)}{\frac{k_{\text{A}}^2}{2m} - W_{\text{A}} - \Delta + \frac{i\Gamma}{2}} \qquad (3)$$

The underlying physics can be described in the language of a full scattering process, where the Auger decay is a resonance in the double photoionization cross-section [28]. The inelastic scattering of the SXR photon γ off an argon atom leads to the formation of an Ar^{2+} dication and the emission of two electrons e_{P}^- and e_{A}^-. Mediated by a set of intermediate states $\{\Phi\}$, it can be represented schematically as

$$\text{Ar} + \gamma \rightarrow \{\Phi\} \rightarrow \text{Ar}^{2+} + e_{\text{P}}^- + e_{\text{A}}^- \qquad (4)$$
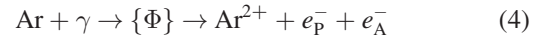
Assuming singly-ionized resonance states $\{\Phi\}$ the photon scattering process (4) can be separated into two parts. First, the FEL pulse with photon energy Ω_{FEL} excites a core electron from the 2p shell with binding energy E_0 to a continuum state with energy $W_{\text{P}} = E_0 + \Omega_{\text{FEL}}$ (photoionization). Second, the core-hole vacancy is filled with a valence electron from the energy level E_{a}. The excess energy is transferred ultrafast by electron correlation to a second valence electron and the Auger electron is emitted from the corresponding energy level E_{b} to a continuum state with energy $W_{\text{A}} = E_{\text{a}} + E_{\text{b}} - E_0$ (subsequent electronic Auger decay).

In this two-step model, the energy shift of the resonance state Δ and the Auger line width Γ can be calculated in second-order perturbation theory and by Fermi's golden rule, respectively [26]. Of course, the related core-hole lifetime must enter any theoretical description of the processes because it affects both creation and interference of propagating Auger electron wave packets. However, the measurement itself and our presentation of the data are oblivious to it. The spectral shape of the two-electron function is determined by the exponential Auger decay resulting in a Lorentzian line profile and the spectral envelope $\tilde{\mathcal{E}}_{\text{FEL}}$ of the FEL double pulse. The latter can be described by

$$\tilde{\mathcal{E}}_{\text{FEL}}(\tau, \omega) = \sqrt{\frac{\pi}{2 \log 2}} \tilde{\mathcal{E}}_{\text{FEL}}^0 \tau_0 \, e^{-\frac{\omega^2 \tau_0^2}{8 \log 2}} \left(1 + e^{i\omega\tau}\right) \qquad (5)$$

where $\tilde{\mathcal{E}}_{\text{FEL}}^0$ and τ_0 denote the FEL peak electric field strength and the individual FEL pulse duration, respectively. The energy balance of the correlated two-electron process enters in the argument of $\tilde{\mathcal{E}}_{\text{FEL}}$ in equation (3). For monochromatic

SXRs with photon energy Ω_{FEL}, i.e. a continuous wave sources one derives

$$\frac{k_P^2}{2m} + \frac{k_A^2}{2m} = \Omega_{FEL} - I^{2+} = \Omega_{FEL} + E_a + E_b \qquad (6)$$

Here, I^{2+} is the double-ionization potential of a neutral Ar atom for producing the dicationic final state.

The basic experimental observable in the present study is the probability density $\left| c_f^{\vec{k}_P \vec{k}_A}(\tau) \right|^2$ to find the quantum system in the dicationic final state with a photoelectron of momentum $\vec{k}_P$ and an Auger electron of momentum $\vec{k}_A$ as a function of the time delay between the two pulses.

Let us first consider the case of 2p photoelectron detection. Within the above-described *ab initio* formalism based on [27], the probability density to observe a photoelectron with momentum $\vec{k}_P$ is given by

$$P\left(\tau, \vec{k}_P\right) \propto \left| \bar{d}\left(\vec{k}_P\right) \right|^2$$
$$\times \int_{-\infty}^{\infty} \text{Im} \left[\frac{\left| \tilde{\mathcal{E}}_{FEL}(\tau, \omega) \right|^2}{\frac{k_P^2}{2m} - W_P + \Delta - \omega - \frac{i\Gamma}{2}} \right] d\omega$$
$$(7)$$

It results from the integration of the probability density of equation (2) over the unobserved degrees of freedom, which is in this case the Auger electron momentum $\int \int \int \left| c_f^{\vec{k}_P \vec{k}_A}(\tau) \right|^2 d^3 k_A$. Note that in our experiment we did not measure the kinetic energy distribution of direct photoelectrons in coincidence with the Auger electrons. From this analysis, one can see in equation (7) that the interference of the 2p photoelectrons is caused by the spectral envelope $\tilde{\mathcal{E}}_{FEL}$ of the (relative) phase-locked coherent FEL pulse replicas.

Next, we turn to the theoretical description of the Auger electron interference. Along the lines discussed above, in this case we need to integrate the probability density (2) over the photoelectron momentum. One derives

$$P\left(\tau, \vec{k}_A\right) \propto \left| \bar{q}\left(\vec{k}_A\right) \right|^2$$
$$\times \int_{-\infty}^{\infty} \text{Im} \left[\frac{\left| \tilde{\mathcal{E}}_{FEL}(\tau, \omega) \right|^2}{\frac{k_A^2}{2m} - W_A + \Delta - \omega - \frac{i\Gamma}{2}} \right] d\omega \quad (8)$$

Again, we can see that the interference of the Auger electrons should be exclusively caused by the spectral envelope $\tilde{\mathcal{E}}_{FEL}$ of the FEL pulse replicas. It explains why the interferometric trace of the 'normal' $L_{2,3}M_{2,3}M_{2,3}$ Auger decay multiplet follows that of the $L_{2,3}$ photo lines shown in figures 3(a) and (c), respectively.

At this point, we are still left with the key question: what is the origin of the relative phase delay of the $L_{2,3}M^3$ satellite transitions with respect to the oscillation of the driving SXR light wave, i.e. where does the corresponding 3 attosecond delay observed in figure 3 come from? Let us have a look at some of the approximations that enter into the ab-initio formalism to describe the inelastic scattering process in the essential

state model [28]: (i) electron correlations in the ground-state of the neutral Ar atom, the Ar^+ cation, and the Ar^{2+} dication are not included. (ii) Coulomb repulsion between the outgoing photo and Auger electron (postcollision interaction [19, 29]) is neglected. (iii) The interaction between the outgoing electrons and the remaining ground-state electrons is not taken into account. The first two processes should also affect (at least to some extent) the normal Auger emission in a similar way as they modify the shake-up induced spectator decay and therefore cannot fully account for the observed relative-phase difference between the two. The third process however is at the heart of the shake-up mechanism itself. Therefore, a full theoretical description of the observed phenomena must include the Coulomb interaction of the ejected electrons with the bound electrons of the remaining quantum system. Their inelastic interaction creates additional resonance states $\{\Phi\}$ in the full scattering process represented by scheme (4), which certainly includes correlated two-hole one-particle (2h1p) excitations. These electronic configurations open up the spectator decay channels into final shake-up states ($L_{2,3}M^3$), which we tracked with attosecond precision in the present experiment. It is important to note that the propagation of an ionized electronic wave packet through the attractive ionic Coulomb potential can also be viewed as a (half-)scattering process, which leads to an energy-dependent phase shift as compared to its free propagation in vacuum [30–32]. Any time-dependent modification of the ionic potential due to the mutual interaction of electrons and their correlated motion will affect this phase shift and this holds for both, the Auger as well as the direct photoelectron emission. Figure 4 sketches the different electronic excitation and relaxation channels populated in the inelastic scattering process with the FEL double pulse at the central wavelength of 4.5 nm (274.7 eV) upon 2p hole formation in argon atoms.

From the discussion, we conclude that the observed relative phase delay of the $L_{2,3}M^3$ satellite transitions with respect to the normal $L_{2,3}M_{2,3}M_{2,3}$ Auger decay reflects the many-body correlations of the intermediate shake-up states $\{\Phi\}$. In particular, those properties of the time-dependent electronic structure affecting the Coulomb interaction matrix elements between the intermediate and final states are of importance. For instance, the excited nl-Rydberg states of the ion resulting from the shake-up transition are strongly polarizable due to their large spatial extent compared to the ionic ground state. Recently, it was shown by attosecond streaking spectroscopy that the resulting effective dipole exerts a back action on the outgoing electron [33]. It leads to a time shift of the electron ejected from the helium ground state by an extreme-ultraviolet photon, either leaving the ion in its ground state or exciting it into a shake-up state. Depending on the photon energy the authors observed 3–6 attosecond retardation of the emitted photoelectron wave packet due to electronic correlations, which is the same order of magnitude of what we found in the present work.

4. Summary and outlook

Pilot experiments to clock SXR induced correlated electron dynamics with time-domain interferometry provide novel
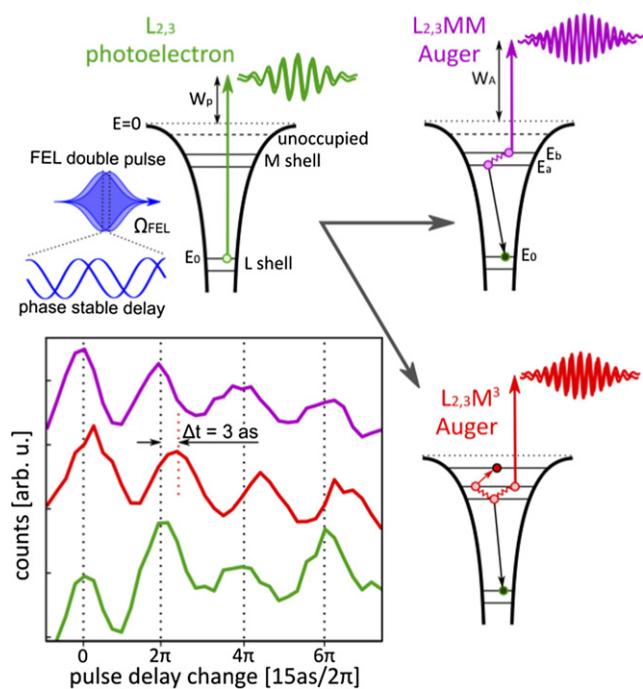
Figure 4. Schematic of argon 2p core hole formation (green) with subsequent Auger decay. Dynamic information is gained by electron wave packet interferometry comparing normal $L_{2,3}M_{2,3}M_{2,3}$ Auger decay (without spectator hole, purple) with the spectator decay into final shake-up states ($L_{2,3}M^3$, red). Only participating electrons are drawn. The kinetic energy of the Auger- and photoelectrons is detected in a magnetic bottle electron spectrometer. Integrated interferometric traces of electron emission for different kinetic energy ranges: 24–29 eV (green), 140–160 eV (red) and 190–210 eV of ejected electrons are shown. It is the same data set as presented in figure 3.

information on the variation of the scattering phase in argon 2p core-hole relaxation processes. The phase-sensitive detection of the emitted electrons turns electron spectroscopy for chemical analysis (ESCA), developed by Kai Siegbahn in the early 1970s [34], into a new age of quantum interferometry for resolving non-equilibrium electron dynamics (QUINED) on ultrafast time scales introduced in the present paper. Specific non-radiative Auger decay channels, namely the $L_{2,3}M^3$ satellite transitions into final shake-up states, show a relative time (phase) delay of 3 attoseconds with respect to the driving SXR light wave oscillation and the normal $L_{2,3}M_{2,3}M_{2,3}$ Auger decay (without spectator hole), respectively. This is among the fastest electronic processes ever measured demonstrating the power of phase-sensitive detection of interaction products using coherent SXRs.

The FEL pulses applied in the present study exhibit a spectral bandwidth of $\approx \frac{1.8}{\sqrt{2}}$ eV full-width-at-half-maximum intensity at the central photon energy of 274.7 eV (see figure 1, inset). This is on the order of the spin–orbit splitting of the 2p core hole state (≈ 2.1 eV) and in turn, a coherent superposition of the cationic eigenstates is populated, at least to some extent. Furthermore, the spectral bandwidth of the coherent SXR FEL pulse is large compared to the energy difference of individual shake-up states (see figure 2, inset), thus

allows for excitation of multiple shake-up resonances simultaneously. As a consequence, a fully coherent bound electronic wave packet that features rapid multi-state quantum beating is formed. The energies of emitted electrons can be identical upon inelastic SXR scattering and electrons with the same linear momentum interfere. A released electron wave packet may also consist of two or more partial waves, with different angular momenta and phases. Since their angular distributions are different, these partial waves may also interfere, introducing anisotropy in the angular distribution [4]. All of these quantum interferences may trigger beating structures in the recorded time-dependent interferometric traces and the first indications might be visible already in figures 3 and 4.

A full characterization of the multi-electron Auger shake-up dynamics with improved electron kinetic energy resolution, longer acquisition times for better statistics, and longer time scans will provide a novel benchmark for the test and development of multi-electron theories for more complex systems. The many-body problem of electronic correlations is among the grand challenges across different research areas ranging from atomic and molecular physics via chemistry to condensed matter and materials science. Specifically in the latter areas, a detailed understanding of these processes could shed new light on many highly relevant phenomena that are mediated by electronic correlations, for example, topological phases, phase transitions, magnetism, or superconductivity.

Acknowledgments

ORCID iDs

Karolin Baev https://orcid.org/0000-0002-0146-6318
Marie Kristin Czwalinna https://orcid.org/0000-0002-7651-4660
Andreas Hans https://orcid.org/0000-0002-4176-4766
Steffen Palutke https://orcid.org/0000-0001-8693-2674
Jens Viefhaus https://orcid.org/0000-0003-1154-0750
Michael Martins https://orcid.org/0000-0002-1228-5029
André Knie https://orcid.org/0000-0002-2208-8838
Tim Laarmann https://orcid.org/0000-0003-4289-8536

References

[1] Auger P 1925 *Compt. Rend.* **180** 65
[2] Krausz F and Ivanov M 2009 *Rev. Mod. Phys.* **81** 163
[3] Wituschek A *et al* 2020 *Nat. Commun.* **11** 883
[4] Pazourek R, Nagele S and Burgdörfer J 2015 *Rev. Mod. Phys.* **87** 765
[5] You D *et al* 2019 arXiv:1907.13605
[6] Pabst S and Dahlström J M 2016 *Phys. Rev. A* **94** 013411
[7] Klünder K *et al* 2011 *Phys. Rev. Lett.* **106** 143002
[8] Guénot D *et al* 2014 *J. Phys. B: At. Mol. Opt. Phys.* **47** 245602
[9] Gúenot D *et al* 2012 *Phys. Rev. A* **85** 053424
[10] Palatchi C, Dahlström J M, Kheifets A S, Ivanov I A, Canaday D M, Agostini P and DiMauro L F 2014 *J. Phys. B: At. Mol. Opt. Phys.* **47** 245003
[11] Kheifets A S 2013 *Phys. Rev. A* **87** 063404
[12] Schultze M *et al* 2010 *Science* **328** 1658
[13] Eckle P, Pfeiffer A N, Cirelli C, Staudte A, Dorner R, Muller H G, Buttiker M and Keller U 2008 *Science* **322** 1525
[14] Eckles P, Smolarski M, Schlup P, Biegert J, Staudte A, Schöffler M, Muller H G, Dörner R and Keller U 2008 *Nat. Phys.* **4** 565
[15] Pfeiffer A N *et al* 2012 *Nat. Phys.* **8** 76
[16] Pfeiffer A N, Cirelli C, Smolarski M, Dörner R and Keller U 2011 *Nat. Phys.* **7** 428
[17] Paul P M *et al* 2001 *Science* **292** 1689
[18] Loriot V *et al* 2017 *J. Opt.* **19** 114003
[19] Armen G B, Aksela H, Åberg T and Aksela S 2000 *J. Phys. B: At. Mol. Opt. Phys.* **33** R49
[20] Usenko S *et al* 2017 *Appl. Sci.* **7** 544
[21] Usenko S *et al* 2017 *Nat. Commun.* **8** 15626
[22] Faatz B *et al* 2016 *New J. Phys.* **18** 062002
[23] Brünken S *et al* 2002 *Phys. Rev. A* **65** 042708
[24] Nakano M *et al* 2012 *Phys. Rev. A* **85** 043405
[25] Carroll T X, Bozek J D, Kukk E, Myrseth V, Sæthre L J and Thomas T D 2001 *J. Electron Spectrosc. Relat. Phenom.* **120** 67
[26] Smirnova O, Yakovlev V S and Scrinzi A 2003 *Phys. Rev. Lett.* **91** 253001
[27] Buth C and Schäfer K J 2015 *Phys. Rev. A* **91** 023419
[28] Buth C and Schäfer K J 2009 *Phys. Rev. A* **80** 033410
[29] Saha H P 1990 *Phys. Rev. A* **42** 6507
[30] Wigner E P 1955 *Phys. Rev.* **98** 145147
[31] Eisenbud L 1948 *PhD Thesis* Princeton University
[32] Smith F T 1960 *Phys. Rev.* **118** 349
[33] Ossiander M *et al* 2017 *Nat. Phys.* **13** 280
[34] Siegbahn K, Hammond D, Fellner-Feldegg H and Barnett E F 1972 *Science* **176** 245